

## DIRECTIONAL DEPENDENCE OF $\Lambda$ CDM COSMOLOGICAL PARAMETERS

M. AXELSSON<sup>1</sup>, Y. FANTAYE<sup>1</sup>, F. K. HANSEN<sup>1</sup>, A. J. BANDAY<sup>2</sup>, H. K. ERIKSEN<sup>1</sup>, K. M. GORSKI<sup>3,4,5</sup>

*Draft version March 24, 2018*

### ABSTRACT

We study hemispherical power asymmetry (Eriksen et al. 2004; Hansen et al. 2004; Hansen et al. 2009) in the WMAP 9-year data. We analyse the combined V- and W-band sky maps, after application of the KQ85 mask, and find that the asymmetry is statistically significant at the  $3.4\sigma$  confidence level for  $\ell = 2\text{--}600$ , where the data is signal dominated, with a preferred asymmetry direction  $(l, b) = (227, -27)$ . Individual asymmetry axes estimated from six independent multipole ranges are all consistent with this direction. Subsequently, we estimate cosmological parameters on different parts of the sky and show that the parameters  $A_s$ ,  $n_s$  and  $\Omega_b$  are the most sensitive to this power asymmetry. In particular, for the two opposite hemispheres aligned with the preferred asymmetry axis, we find  $n_s = 0.959 \pm 0.022$  and  $n_s = 0.989 \pm 0.024$ , respectively.

*Subject headings:* cosmic microwave background — cosmology: observations — methods: statistical

### 1. INTRODUCTION

Shortly after the release of the first-year WMAP data (Bennett et al. 2003), Eriksen et al. (2004) and Hansen et al. (2004) reported a detection of a hemispherical power asymmetry in the cosmic microwave background (CMB) on large angular scales in the multipole range  $\ell = 2\text{--}40$ . The power in this multipole range was found to be significantly higher in the direction towards Galactic longitude and latitude  $(l = 237^\circ, b = -20^\circ)$  than in the opposite direction. Due to computational limitations at the time, higher multipoles were not investigated. These findings were supported by numerous other studies, e.g., Park (2004); Hansen et al. (2009) and references therein. However, the significance of the results has often been called into question, in particular, due to the alleged a-posteriori nature of the statistics used. In particular, it is debated whether the statistic has been designed to focus on visually anomalous features revealed by an inspection of the data (e.g., Bennett et al. 2011).

The only rigorous way to contend with this assertion is by performing repeated experiments and analysing the resulting independent data sets that may provide additional information. For cosmological studies, this is in general difficult, given that there is only one available Universe. However, it is not impossible — the standard inflationary cosmological model assumes that the Universe is homogeneous and isotropic, and that the initial fluctuations have amplitudes that are Gaussian distributed, independent and with random phase. This implies that different physical scales should be statistically uncorrelated, and therefore the morphology of the largest scales should not have any predictive power over the mor-

phology of the smaller scales. For the power asymmetry, this suggests that there is a possibility to study effectively new data sets by considering angular scales that have not previously been studied.

This extension to smaller angular scales was first undertaken by Hansen et al. (2009), when analyzing the WMAP 5-year temperature data set. The asymmetry was then found to extend over the range  $\ell = 2\text{--}600$  with a preferred direction  $(l = 226^\circ, b = -17^\circ)$  for the higher multipoles, fully consistent with the direction for the lower multipoles found in the original 1-year WMAP analysis. Two approaches were used for the analysis: (1) a statistical model selection procedure taking into account the penalty for including 3 new parameters (amplitude and direction of asymmetry), which showed that indeed an asymmetric model was preferred; and (2) a simple test in which the preferred power asymmetry axis was estimated independently for six multipole bins of width  $\Delta\ell = 100$ . It was found that these directions, which should be statistically independent, were strongly aligned; none of the 10000 simulated isotropic CMB maps showed a similarly strong clustering of preferred directions. An alternative approach modeled the power asymmetry in terms of a dipolar modulation field, as suggested by Gordon et al. (2005). Hoftuft et al. (2009) found a  $3.3\sigma$  detection using data smoothed to an angular resolution of  $4.5^\circ$  FWHM, with an axis in excellent agreement with previous results. These studies, covering very different angular scales than those used in the original analysis, argue against an a-posteriori interpretation of the effect.

In this Letter, we repeat the high- $\ell$  analysis due to Hansen et al. (2009) using the WMAP<sup>6</sup> 9-year data (hereafter referred to as WMAP9, with a similar notation for the first- and five-year data sets). However, the main goal is to estimate cosmological parameters in the two maximally asymmetric hemispheres, in order to assess their stability with respect to the power asymmetry (for a closely related theoretical study, see Moss et al. 2011, and references therein.). A similar analysis was performed in Hansen et al. (2004) using the WMAP first-

magnus.axelsson@astro.uio.no

y.t.fantaye@astro.uio.no

<sup>1</sup> Institute of Theoretical Astrophysics, University of Oslo, P.O. Box 1029 Blindern, N-0315 Oslo, Norway

<sup>2</sup> Universite de Toulouse, UPS-OMP, IRAP, Toulouse, France

<sup>3</sup> Jet Propulsion Laboratory, M/S 169/327, 4800 Oak Grove Drive, Pasadena CA 91109

<sup>4</sup> Warsaw University Observatory, Aleje Ujazdowskie 4, 00-478 Warszawa, Poland

<sup>5</sup> California Institute of Technology, Pasadena CA 91125

<sup>6</sup> <http://www.lambda.gsfc.nasa.gov>

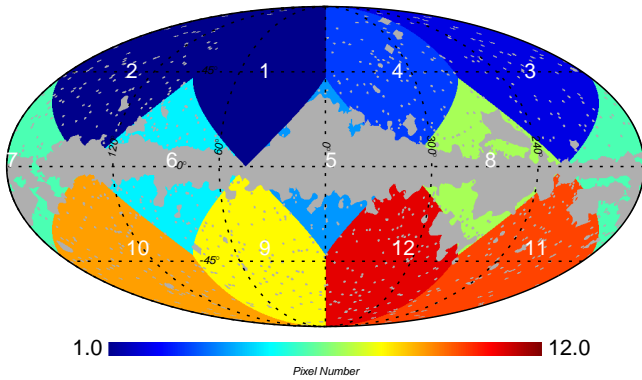


FIG. 1.— The 12 sky patches used in this paper: the regions are delineated by the intersection of the 12 HEALPix base pixels with the WMAP9 KQ85 mask.

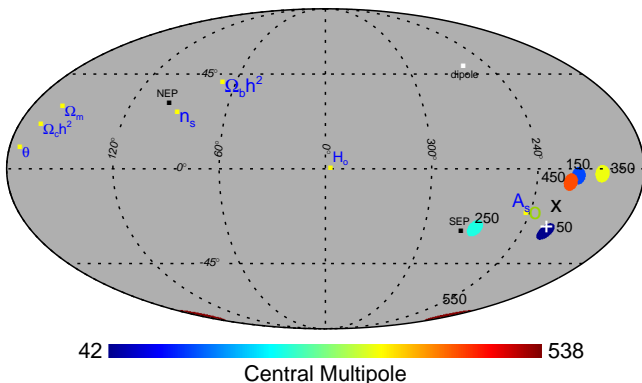


FIG. 2.— Dipole directions for maps of the local power spectrum computed for the 12 regions in Figure 1 from the WMAP9 combined V- and W-band data and separated into six 100-multipole bins. We also show the direction for the full  $\ell = 2 - 600$  range (white cross), for the  $\ell = 2 - 40$  interval determined from WMAP1 (green circle) and the  $\ell = 2 - 600$  range from WMAP5 (black cross). NEP and SEP denote the North and South Ecliptic Poles, respectively. The dipole directions for the local parameter estimate maps are also shown.

year data, but only taking into account the asymmetry observed in the  $\ell = 2 - 40$  range, limited by a grid-based approach, and consequently only considering a few cosmological parameters. In the following, we use CosmoMC<sup>7</sup> to obtain the full posterior of all relevant cosmological parameters using the entire multipole range afforded by the WMAP9 data. We adopt canonical  $\Lambda$ CDM as our baseline cosmological model, with six parameters - the baryon density today  $\Omega_b h^2$ , the Cold dark matter density today  $\Omega_{DM} h^2$ , the scalar spectrum power-law index  $n_s$ , the log power of the primordial curvature perturbations  $\log[10^{10} A_s]$ , the angular size of the sound horizon at recombination  $\theta$ , and the Hubble constant  $H_0$ , where  $h$  represents this value in units of  $100 \text{ km s}^{-1} \text{ Mpc}^{-1}$ .

## 2. DATA AND METHOD

We use the publicly available WMAP9 temperature sky maps (Bennett et al. 2012), co-adding (with inverse-noise-variance weighting) the V (61 GHz) and W (94 GHz) band foreground-cleaned maps. We also generate a set of 10000 simulated CMB-plus-noise Monte

<sup>7</sup> COSMOlogical Monte Carlo software package (<http://www.cosmologist.info/cosmomc>).

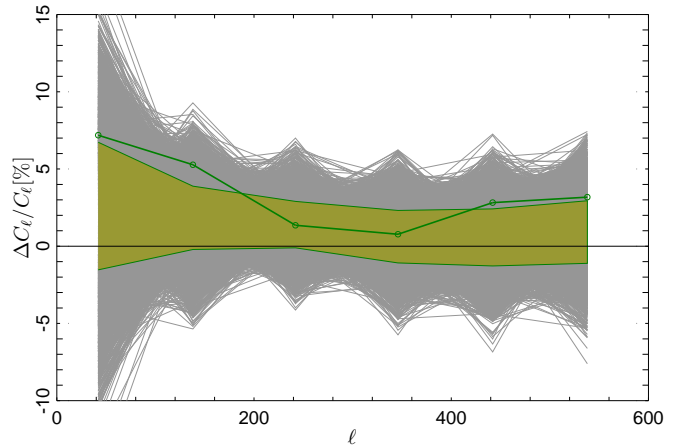


FIG. 3.— The ratio of the local power spectra computed from antipodal hemispheres centred along the preferred dipole direction, as determined over the  $\ell = 2 - 600$  range. The connected dark-green open circles correspond to the values derived from the WMAP9 coadded V- plus W-band data. The grey lines are the individual power spectra ratios as computed for the preferred dipole direction of each of the 10000 simulations. The olive-green band with dark-green bounding curves represents the corresponding 68% confidence levels.

Carlo (MC) simulations based on the WMAP best-fit  $\Lambda$ CDM power spectrum (Hinshaw et al. 2012), noise rms maps and beam profiles for the V and W bands. The WMAP9 KQ85 Galactic and point source mask is used to remove pixels with high foreground contamination.

*Power asymmetry:* — The MASTER (Hivon et al. 2002) approach is used to estimate the power spectra,  $C_\ell$ , from pseudo-spectral estimators applied to local regions of the sky. When computing the MASTER kernel, we bin the pseudo-spectra into bins of width  $\Delta\ell = 16$  in order to avoid a singular matrix. This version of the spectra is used later for parameter estimation.

In order to estimate the dipole directions of the local spectra, we first obtain an  $N_{\text{side}} = 1$  map, as illustrated in Figure 1, where the value of each pixel is the binned power spectrum for a given range in  $\ell$ . However, in this case we combine the  $16\ell$ -bins further into blocks containing approximately 100 multipoles, following the procedure used in Hansen et al. (2009), and thereby reducing the uncertainty on the direction. From this map we then estimate the dipole amplitude and direction using an inverse variance weighting of the pixels; the variance of each pixel is calculated using 10000 isotropic simulations which incorporate the noise and beam properties of the data, and to which the same mask has been applied.

For an isotropic map, the power spectrum should be uncorrelated between multipoles. Although masking does introduce correlations between adjacent multipoles, it is not expected that this will be significant between the 100-multipole blocks, and therefore the dipole directions should be random. This is confirmed by simulations. The degree of alignment between the dipole directions of different multipole blocks is then used as a measure of the power spectrum asymmetry.

We also use the 100-multipole blocks to compute the power spectra for the two opposite hemispheres defined by the direction of maximum asymmetry, and for disks of diameter 90 degrees centered on the same directions.

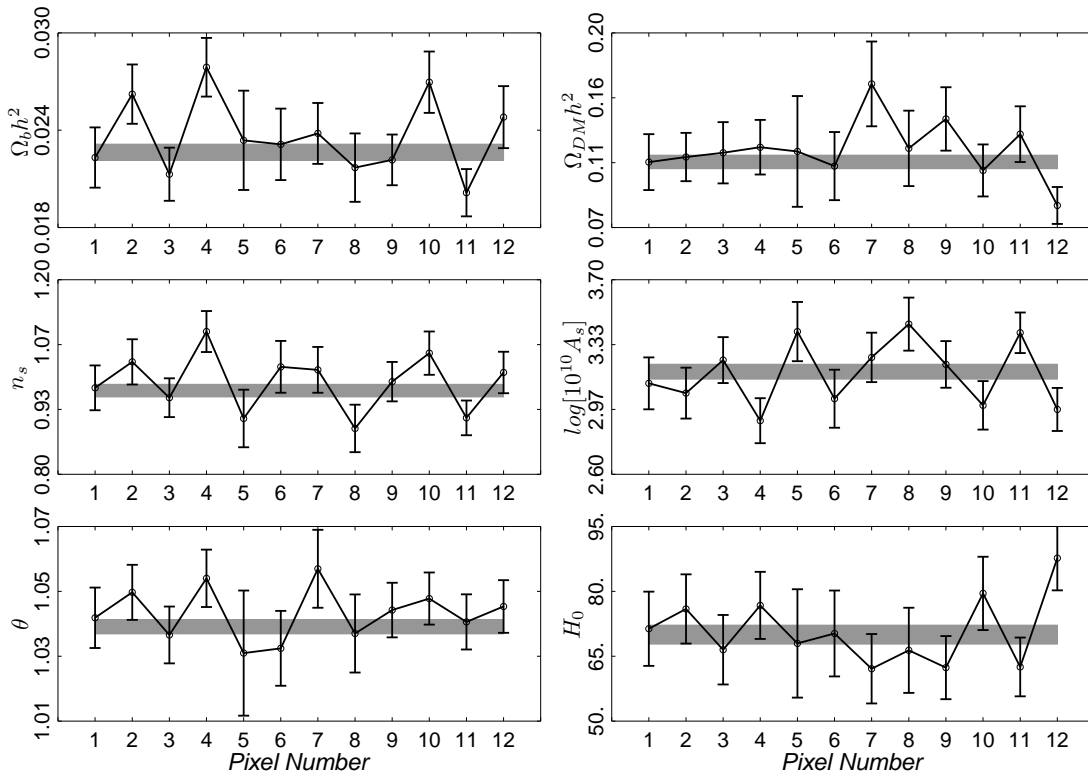


FIG. 4.— Estimated  $\Lambda$ CDM parameter values for the 12 regions defined in Figure 1, as indicated by the open circles. The estimates are based on multipoles in the range  $\ell = 2 - 1008$ . The grey band represents the 68% confidence level determined from a likelihood analysis of the WMAP9 data with the KQ85 mask applied.

*Cosmological parameter estimation:*— Our primary interest here is to evaluate the directional dependence of the cosmological parameters in the temperature data. We apply a similar binning and power spectrum estimation method as described above. For the high- $\ell$  likelihood, we compute the MASTER estimates of the spectra from the full-resolution  $N_{\text{side}} = 512$  map. For the low- $\ell$  likelihood, we replace the WMAP pixel likelihood by a MASTER estimate computed for a single bin,  $\ell \in [2, 31]$ . Tests indicate that this modification does not introduce any significant deviation in the parameters on the full sky as compared to the official WMAP values. Indeed, the parameter estimate changes were insignificant when compared to each parameter’s  $1\sigma$ -value. The maximum multipole used in the parameter analysis is  $\ell_{\text{max}} = 1008$ . For all spectra, we subtract the best-fit unresolved point source amplitude (Hinshaw et al. 2012) before parameter estimation.

Our TT likelihood code uses the offset log-normal term that was introduced into the WMAP likelihood in Verde et al. (2003) - hence the total likelihood is a linear combination of Gaussian and log-normal terms:

$$-\log \mathcal{L}(C_b | \widehat{C}_b) \sim \frac{1}{3} \sum_{b,b'} \Delta C_b C_{bb'}^{-1} \Delta C_b^T + \frac{2}{3} \sum_{b,b'} \Delta z_b \mathcal{Q}_{bb'} \Delta z_b^T \quad (1)$$

where  $\widehat{C}_b$  and  $C_b$  are the estimated and model power spectra respectively,  $\Delta C_b = C_b - \widehat{C}_b$ ,  $C_{bb'}^{-1}$  is the covariance matrix, estimated using CMB plus noise MC simulations,  $z_b = \ln(C_b + N_b)$ , (where  $N_b$  is the noise spectrum) and  $\mathcal{Q}_{bb'} = (\widehat{C}_b + N_b) C_{bb'}^{-1} (\widehat{C}_{b'} + N_{b'})$  is the local transformation of the covariance matrix to the log-normal variables

$z_b$ . The last term is added since a simple Gaussian likelihood does not capture the full likelihood surface. A linear combination of Gaussian+Log-normal terms has been tested and proven to be minimally biased by the WMAP team (Verde et al. 2003). The transformation to  $z_b$  variables introduces no extra bias in the variance by construction, and this implies the stated relationship between  $C^{-1}$  and the curvature matrix  $\mathcal{Q}$ . For further details see Bond et al. (1998).

To construct the covariance matrix, we use 10 000 CMB plus noise Gaussian simulations. The covariance matrix propagates the uncertainties introduced by effects such as the noise, mask geometry, and associated sample variance. We make no attempt to include beam uncertainties in our pipeline.

The fractional areas of the 12  $N_{\text{side}} = 1$  patches range from  $f_{\text{sky}} = 0.019$  in the Galactic center to  $f_{\text{sky}} = 0.085$  in regions at high latitude. With such small patches, one might be concerned about the correctness of our likelihood approximation. We have confirmed that the parameter estimates are unbiased, performing parameter estimation on some of the small regions in 500 simulated maps with known input parameters.

The final posterior distribution is comprised of the product of the likelihood and a prior distribution that describes our previous knowledge of the parameters. Since we do not consider polarization in our analysis, we adopt a strong Gaussian prior on the reionization redshift,  $z_{\text{rei}} = 10.6 \pm 1.1$ , which corresponds to the WMAP9 best-fit value. Due to the strong correlation of  $z_{\text{re}}$  and the reionization optical depth  $\tau$ , we can also obtain an additional constraint on this parameter as well. We also used the CosmoMC default hard-coded priors on the Hubble

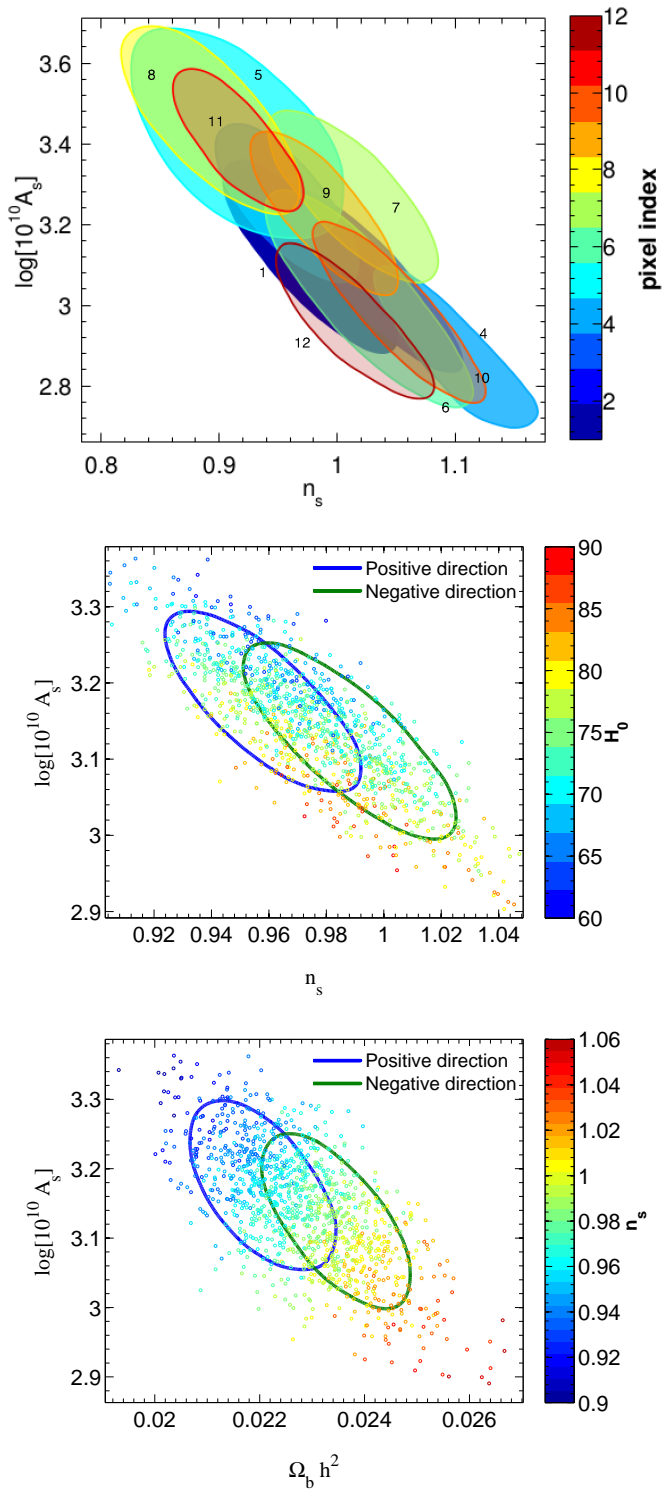


FIG. 5.— *Top*: Summary of the  $n_s$ – $\log(10^{10} A_s)$  posterior in terms of  $1\sigma$  contours for the 12 regions. *Middle*: As above, but evaluated from antipodal hemispheres aligned with the preferred asymmetry direction. Colored dots indicate the values of  $H_0$ . *Bottom*: As the middle plot, but for  $\Omega_b h^2$ – $\log(10^{10} A_s)$ .

constant and age of the Universe. The flat priors used in the other cosmological parameters is wide enough that the final estimates are dominated by the data.

### 3. RESULTS

*Power asymmetry:* — In Figure 2, we show the dipole directions of the first six 100-multipole bands as estimated from the corresponding  $N_{\text{side}} = 1$  maps constructed from the 12 local power spectrum estimates, together with the dipole for the full multipole range  $\ell = 2 - 600$ . These directions are consistent with those found from the WMAP1 (Hansen et al. 2004) and WMAP5 (Hansen et al. 2009) data sets, which are also indicated in the figure.

For a statistically isotropic CMB temperature distribution, the dipole directions from uncorrelated power spectrum estimates should be distributed randomly on the sky. To quantify the significance of the power asymmetry, we consider the dispersion angle, which is defined as the mean angle,  $\theta_{\text{mean}}$ , between all possible combinations of 100-multipole dipole directions up to a given  $\ell_{\text{max}}$ . The expected dispersion angle for Gaussian simulations is 90 degrees, as confirmed by simulations. We calculate  $\theta_{\text{mean}}(\ell_{\text{max}} = 600)$  for the WMAP9 data and compare it to the distribution obtained from 10 000 CMB plus noise simulations. We found that only 7 of these exhibited a lower dispersion angle, implying a  $3.4\sigma$  significance for the power asymmetry. This is lower than previously reported in Hansen et al. (2009), where none of the 10 000 simulations had a similarly large mean angle. However, there are several changes in this analysis; (1) the new 9-year Galactic and point source masks remove a larger fraction of the sky, thus increasing the scatter on the dipole directions due to increased sample variance; (2) larger disks are now used since the smaller disks from the 5-year analysis result in several patches near the Galactic center with an extremely small sky fraction when combined with the new Galactic mask; and (3) 12 independent regions are now used instead of 3072 overlapping ones to speed-up the computations. It is also interesting to note that we have tried a number of permutations of the individual yearly sky maps and found variations depending on which particular years were excluded. However, the results always remain highly significant, and the variations are found to be consistent with those determined from simulations.

In order to illustrate the effect of the asymmetry on the power spectrum, we show in Figure 3 the ratio  $\Delta C_\ell / C_\ell$  of the power spectrum difference between the two antipodal hemispheres compared to their mean spectrum as computed along the maximum asymmetry direction. The olive-green band shows the 68% confidence limit determined from simulations. Note that the corresponding mean ratio is larger than zero since the maximum asymmetry direction for each single simulation is used. The amplitude of the mean ratio over the range  $\ell = 2 - 600$  for the data is exceeded in only 0.52% of the simulations.

Inspection of Figure 2 suggests that some of the dipole directions are close to the south ecliptic pole. If the asymmetry had its origin in an instrumental systematic effect, or from some local foreground in the Solar System, then one might expect an alignment of the asymmetry with the ecliptic axis. For this reason, we study this relation further. Note first that the distance from the direction of maximum asymmetry to the south ecliptic pole is 44 degrees. We calculated the mean distance of the 6 dipole directions to the ecliptic pole as well as to the axis of maximum asymmetry and compared to simulations. While the mean angular distance to the direction

of maximum asymmetry is smaller than that for the data in only 0.02% of the simulations, the equivalent distance to the ecliptic pole is smaller in 3% of the simulations. Furthermore, the significance of the  $C_\ell$  ratio measured in opposing ecliptic hemispheres is 29%. We therefore conclude that the asymmetry is most likely not related to the ecliptic frame.

Another possible mechanism for generating asymmetry is through the Doppler boosting of the CMB fluctuations due to our motion with respect to the CMB reference frame (see Planck Collaboration et al. 2013, and references therein). This boosting causes a dipolar modulation of the amplitude of the fluctuations and a corresponding hemispherical asymmetry on all scales, and has been observed by *Planck*. It is therefore a strong candidate to produce an alignment of power dipoles as claimed here. However, using simulations we have determined that the magnitude of this effect at the WMAP frequencies is too small to have any impact on the hemispherical asymmetry described in this Letter. The power spectra in opposing hemispheres are changed by a maximum of 0.1% and the mean dipole direction over the range  $\ell = 2 - 600$  is changed by only one degree.

Therefore, we consider if this asymmetry in power is reflected in fits to the standard  $\Lambda$ CDM cosmological parameters.

*Cosmological parameter estimation:*— Figure 4 shows the directional dependence, as specified by the 12 regions on the sky defined in Figure 1 for the six main  $\Lambda$ CDM parameters. The computed values and their standard deviations are shown in black, whilst the corresponding results from our WMAP9 analysis on the full sky with the KQ85 mask applied is shown as a grey band. Inspecting the plots carefully, one finds that the majority of parameter estimates fall within  $\sim 1\sigma$  of the WMAP9 full sky value. One exception is for pixel 4 where there is a  $\sim 3\sigma$  deviation for some parameters. This outlier might be explained by residual foregrounds close to the edge of the mask, or could simply be a large fluctuation.

In Figure 2, we also show the dipole directions of the  $N_{\text{side}} = 1$  parameter maps. Clearly  $n_s$ ,  $A_s$  and  $\Omega_b$  seem to show a directional dependence similar to the power spectrum asymmetry and these seem to be the parameters mostly affected by the asymmetry. Note that the fitted dipole directions for these parameters are only weakly affected by the outlier in pixel 4.

In the left top panel of Figure 5, we demonstrate the  $A_s - n_s$  correlation with  $1\sigma$  contours for each region. All contours are consistent with each other at better than  $2\sigma$ , but some directional dependence is visible.

We also estimated parameters using hemispheres corresponding to the preferred power asymmetry direction for  $\ell = 2 - 600$ . Initially, we restricted the analysis to  $\ell_{\text{max}} = 608$  to cover only that part of the spectrum which is highly signal dominated and where the asymmetry is prominent. However, the absence of higher multipoles leads to large uncertainties in the parameters of interest. We therefore repeated the analysis for  $\ell_{\text{max}} = 1008$ . In

this case, the error ellipses for  $A_s$  vs  $\Omega_b h^2$  and  $A_s$  vs  $n_s$  computed on the positive (power-enhanced) and negative (power-deficit) hemispheres show a slight relative shift, as shown in the bottom panels of Figure 5. The best-fit parameters for each hemisphere lie just at the border or the  $1\sigma$  contours from the opposite hemisphere. The two maximally asymmetric hemispheres do not, therefore, indicate parameter values significantly different from the WMAP9 full-sky results. It is interesting to note that the power-deficit hemisphere prefers in general a higher  $H_0$ . The marginalised value obtained for the scalar spectral index in the two hemispheres is  $n_s = 0.959 \pm 0.022$  and  $n_s = 0.989 \pm 0.024$  respectively (an  $\approx 1.3\sigma$  difference). Note that in one hemisphere, the spectral index is different from 1 at almost  $2\sigma$  whereas in the other it is fully consistent with 1.

In addition, we compared the difference in parameter estimates between the two opposite maximally asymmetric hemispheres of the data to the corresponding CosmoMC estimates in 100 isotropic simulations. In this way we were able to obtain a significance of asymmetry for each single parameter. We found that the p-values for asymmetry in  $\Omega_b h^2$ ,  $\Omega_{DM} h^2$ ,  $n_s$ ,  $\log[10^{10} A_s]$ ,  $\theta$ ,  $H_0$  are 32%, 43%, 53%, 39%, 56%, and 68%, respectively, confirming that no asymmetry is seen in the parameters.

#### 4. CONCLUSIONS

We measure a statistically significant power spectrum asymmetry in the WMAP9 temperature sky maps with  $3.4\sigma$  significance as measured by the mean dispersion among the preferred directions derived from six (nearly) independent multipole ranges between  $\ell = 2$  and 600, using the conservative KQ85 mask adopted in the WMAP9 analysis. Only 7 out of 10 000 simulations show a similarly strong alignment. The average preferred direction points toward Galactic coordinates  $(l, b) = (226, -27)$ ,  $44^\circ$  away from the south ecliptic pole arguing against the possibility of a systematic or local astrophysical cause for the asymmetry related to the ecliptic frame of reference. Conversely, the cosmological parameters do not show a strong regional dependence, although the parameters  $A_s$ ,  $n_s$  and  $\Omega_b$  do hint at a weak sensitivity to the hemispherical power asymmetry.

FKH acknowledges OYI grant from the Norwegian research council. HKE acknowledges supported through the ERC Starting Grant StG2010-257080. We acknowledge the use of resources from the Norwegian national super computing facilities NOTUR. Maps and results have been derived using the HEALpix (<http://healpix.jpl.nasa.gov>) software package developed by Górski et al. (2005). Results have been derived using the CosmoMC code from Lewis & Bridle (2002). We acknowledge the use of the LAMBDA archive (Legacy Archive for Microwave Background Data Analysis). Support for LAMBDA is provided by the NASA office for Space Science.

#### REFERENCES

- Bennett, C. L., et al. 2003, ApJS, 148, 1  
 —. 2011, ApJS, 192, 17  
 Bennett, C. L., et al. 2012, arXiv:1212.5225  
 Bond, J. R., Jaffe, A. H., & Knox, L. 1998, Phys. Rev. D, 57, 2117  
 Eriksen, H. K., Hansen, F. K., Banday, A. J., Gorski, K. M., & Lilje, P. B. 2004, ApJ, 605, 14

- Gordon, C., Hu, W., Huterer, D., & Crawford, T. 2005, Phys. Rev. D, 72, 103002
- Górski, K. M., Hivon, E., Banday, A. J., Wandelt, B. D., Hansen, F. K., Reinecke, M., & Bartelmann, M. 2005, ApJ, 699, 759
- Hansen, F. K., Balbi, A., Banday, A. J., & Górski, K. M. 2004, MNRAS, 354, 905
- Hansen, F. K., Banday, A. J., & Górski, K. M. 2004, MNRAS, 354, 641
- Hansen, F. K., Banday, A. J., Gorski, K. M., Eriksen, H. K., & Lilje, P. B. 2009, ApJ, 704, 1448
- Hinshaw, G., et al. 2012, arXiv:1212.5226
- Hivon, E., Górski, K. M., Netterfield, C. B., Crill, B. P., Prunet, S., & Hansen, F. 2002, ApJ, 567, 2
- Hoftuft, J., Eriksen, H. K., Banday, A. J., Gorski, K. M., Hansen, F. K., & Lilje, P. B. 2009, ApJ, 699, 985
- Lewis, A., & Bridle, S. 2002, Phys. Rev., D66, 103511
- Moss, A., Scott, D., Zibin, J. P., & Battye, R. 2011, Phys. Rev. D, 84, 023014
- Park, C. G. 2004, MNRAS, 349, 313
- Planck Collaboration et al. 2013, ArXiv: 1303.5087 (astro-ph.CO)
- Verde, L., et al. 2003, ApJ, 148, 195